

Lab on a Chip

Accepted Manuscript



This is an *Accepted Manuscript*, which has been through the Royal Society of Chemistry peer review process and has been accepted for publication.

Accepted Manuscripts are published online shortly after acceptance, before technical editing, formatting and proof reading. Using this free service, authors can make their results available to the community, in citable form, before we publish the edited article. We will replace this *Accepted Manuscript* with the edited and formatted *Advance Article* as soon as it is available.

You can find more information about *Accepted Manuscripts* in the [Information for Authors](#).

Please note that technical editing may introduce minor changes to the text and/or graphics, which may alter content. The journal's standard [Terms & Conditions](#) and the [Ethical guidelines](#) still apply. In no event shall the Royal Society of Chemistry be held responsible for any errors or omissions in this *Accepted Manuscript* or any consequences arising from the use of any information it contains.



Lab on a Chip

PAPER

A simple multi-well stretching device to induce inflammatory responses of vascular endothelial cells

Received 00th January 20xx,
Accepted 00th January 20xx

DOI: 10.1039/x0xx00000x

www.rsc.org/

Jiasheng Wang,^a Beiyuan Fan,^a Yuanchen Wei,^a Xingmei Suo^{*b} and Yongsheng Ding^{*a}

We herein introduce a novel multi-well stretching device that is made of three polydimethylsiloxane layers, consisting of the top hole-punched layer, middle thin membrane, and bottom patterned layer. It is the first time to use such simple device to supply axisymmetric and nonuniform strains to cells cultured on the well bottoms which are stretchable. These mechanical stimuli can somewhat mimic the stretching status at the bending site of blood vessels where the strains are complicate. In this device, the nonuniform strains to cells are given through the deformation of the membrane from a flat surface to a spherical cap during an injection of certain volume of water into the chamber between the middle membrane and bottom layer. EA.hy926 cells (a human umbilical vein endothelial cell line) were seeded on the well bottoms and exposed to the axisymmetric strains under 5, 10, 15, and 20 % degree of the deformation of the membrane. The cellular responses were characterized in term of cell morphology, cell viability, and expressions of inflammatory mRNAs and proteins. With increasing the degree of the deformation, the cells exhibited an inclination toward the detachment and apoptosis, meanwhile the expressions of the inflammatory mRNAs and proteins showed significant increment, such as MCP-1, IL-8, IL-6 and ICAM-1. These obtained results demonstrate that the inflammatory responses of EA.hy926 cells can be induced by increasing the magnitude of the strains. This simple device provides a useful tool for in vitro investigation on the inflammatory mechanisms related to vascular diseases.

Introduction

The pulsatile blood pressure originates from the heart and drives blood circulation throughout the cardiovascular system, which exerts two kinds of mechanical forces on the vessel wall, namely shear stress and circumferential stretch. These loads (flow and pressure) result in internal stresses and deformation of vessel wall structure, thus trigger the cells of vessel wall releasing a series of biochemical reactants that maintain physiological functions of blood vessel. Under physiologic conditions, a dynamic balance between mechanical stimuli and biological responses is preserved to maintain homeostatic conditions of vessel wall.¹ A perturbation of this balance with high or low mechanical stimuli may lead to physiological adaptation or potential risks of the vessel wall. For example, due to the perturbation involved with the changes in blood pressure under chronic hypertension conditions, the elevated blood pressure causes the extra circumferential stretch on the vessel wall, resulting in endothelial injury which causes a complex interaction among vascular endothelial cells (VECs),

vascular smooth muscle cells, platelets and leukocytes in an inflammatory cascade. It is well known that atherosclerosis has been recognized as a chronic inflammatory disease, which preferentially occur at vascular niches proximal to vessel branches and bends, including aortic arch, ascending and descending aorta, coronary and carotid arteries. In these sites, the blood flow is disturbed and the strain profile is prone to be heterogeneous.^{2,3}

Up to now, numerous stretching devices, either microfluidic devices or conventional devices, have been developed to explore cellular behaviours in response to controlled external stretch.⁴⁻¹⁸ However, most of them emphasized on two-dimension or uniform strain field and required sophisticatedly pneumatic or mechanical control system to provide stretching force to cells. In contrast, we herein have developed an easy-to-manipulate stretching device coupled with a syringe injection pump to provide strain to cells without complex instrumentation. To the best of our knowledge, it is the first time to use three-dimension, axisymmetric, and non-uniform strain profile for mimicking mechanical stimuli at “disturbed” regions (e.g. vascular arches and bends). Moreover, the multi-well configuration of the device enables cells exposed to various strain conditions simultaneously.

In the following experiments, the effects of cyclic axisymmetric strains with the different strengths and durations on the cell morphology, cell viability, and expression of some

^aCollege of Life Sciences, University of Chinese Academy of Sciences, Beijing 100049, China. E-mail: dingysh@ucas.ac.cn; Fax: 86-10-88256079; Tel: 86-10-88256392

^bSchool of information engineering, Minzu University of China, Beijing, 100081, China. E-mail: xingmeisuo@163.com;

Electronic Supplementary Information (ESI) available: [details of any supplementary information available should be included here]. See DOI: 10.1039/x0xx00000x

relatively inflammatory mRNAs and proteins were compared. The obtained results demonstrate that the inflammatory responses of EA.hy926 cells can be successfully induced by using this device. It might be helpful to investigate the mechanisms of vascular inflammation in those disease-prone regions.

Methods

Stretching device and working principle

The device is fabricated with sandwich-like structure containing the three polydimethylsiloxane (PDMS) layers. Figure 1A and 1B is the schematic diagram of a stretchable well in the device and the image of an actual device with 5×5 well array, respectively. The fabrication of the device is described as follows. First, a half-cured PDMS layer (top) was punched to create a multi-hole array and this layer sticks on a half-cured thin membrane (middle, $100 \mu\text{m}$ in thickness) on the wafer to form a multi-well plate. After cured completely in an oven, the multi-well plate was carefully peeled off from the wafer. Then, a prepared layer with the multiple channel and chamber pattern bonded to the bottom side of the multi-well plate via plasma oxidation to form irreversible sealing under the precise well-to-chamber alignment. The working principle of the device is illustrated in Figure 1C. At the beginning of the stretch, the channels and chambers were filled with water and all outlets of the tubes connected to the channels were open to air for a moment to let the well bottom relax to flat. Next, one-side outlets were blocked while another-side outlets were connected to a syringe pump with the multiple units. After certain volume of water was injected into the chambers, the flat surface of the well bottoms became to be spherical cap, resulting in the deformation of the membrane on which the cells were cultured. The cyclic stretch was accomplished by the alternation of the injection and suction of water into and out of the chambers, respectively. The entire instrumentation of the stretching system is described in Figure 1D.

Strain calibration and measurement

With changing from flat surface to spherical cap, the surface exhibits axisymmetric deformation, however, the theoretical characterization of a spherical cap is complicated.¹⁹ As for this stretching device, the elastic membrane (the middle layer) is deformed as spherical cap during certain volume of water injected into chamber. The round shape of the formed spherical surface was verified by the height (z-axial values) of the focus plate of a series of the marked points on a longitude line. The obtained curves exhibited the round shape under the different degrees of the deformation (the data was shown in Figure S-2 of the ESI). As shown in Figure 2, the relationship between the volume or height of a spherical cap and the degree of deformation is described as the equation (1) and (2), respectively (the details of the calculation are showed in the Section 1 of the ESI). Given certain volume or height, the degree of the deformation can be calculated based on the above equations. However, the actual degrees of the deformation are smaller than the calculated values from the equations. This situation is mostly caused by the dead volume which exists in the entire liquid transfer system. Thus, the calibration of the volume of the injected water is necessary to obtain the expected degree of the deformation. According to the height of a formed spherical cap, the actual degree of the deformation of the surface was calculated without depending on the volume of the injected water. Table S-1 of the ESI shows the calibrated volumes of the injected water vs. the expected degrees of the deformation. In this work, the stretching device can provide the degree of the deformation as much as 20 % without causing water leakage. Although the global change in the surface area of the membrane can be obtained through the calculation, the strains applied to the cells on the spherical cap are heterogeneous along with the same longitude direction. In contrast, the strains applied to the cells are identical along with the same latitude direction. To approximately describe the distribution of the strains on an entire spherical cap, we dispersed the flour particles as the marks on the membrane. The distances between two selected

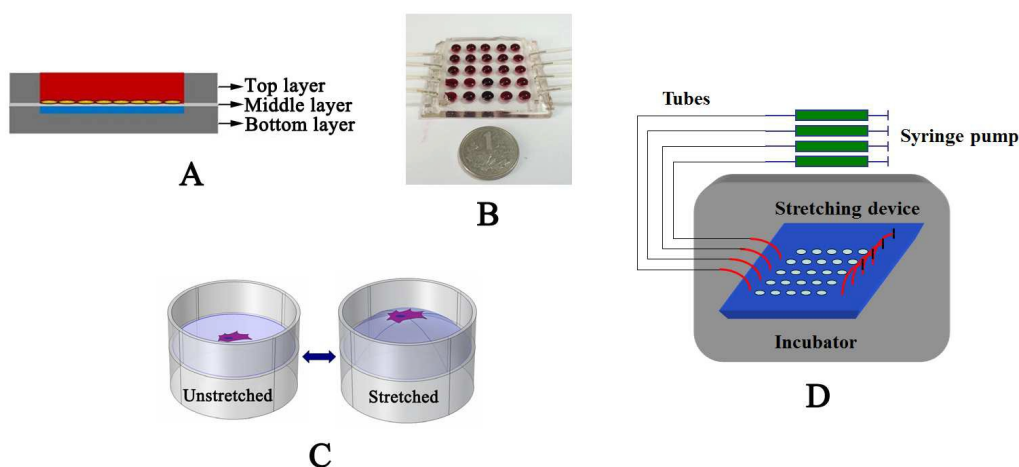


Figure 1. The description of the stretching device. The schematic structure of each well of the device (A); a real device (B); the working principle (C); the profile of the entire stretching system (D).

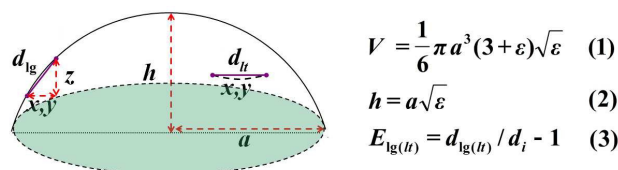


Figure 2. The method for the calculation of strain on a spherical cap. Note: ε is the degree of deformation of membrane; V and h is the volume and height of a spherical cap, respectively; a is the radius of the circle base; E_{lg} and E_{lt} is the strain along with longitude and latitude direction, respectively; d_{lg} and d_{lt} is the distance between two points under the stretched condition along with longitude and latitude direction, respectively. d_i is the initial distance between two points under the unstretched condition; the values of x and y is the displacement between two points along with x axial and y axial at the working platform of a microscopy, respectively. The value of z is the displacement between two focal plates of two points under the stretched condition.

particles were measured during the stretched and unstretched conditions. The magnitudes of the strains along with the longitude and latitude direction were obtained according to the equation (3) in Figure 2. The distance between two particles was limited less than $100 \mu\text{m}$ in order to neglect the curvature effect of spherical cap. Due to the three-dimensional deformation, the distance between two particles along with longitude direction within the intermediate and peripheral regions is difficult to be measured under two-dimensional image. To dissolve this problem, the distance between two particles in a two-dimensional image and z -axial displacement (difference between the focal plane positions of two particles) is treated as two adjacent sides of a right triangle, thus the distance between two particles along with longitude direction is approximately equal to the right-triangle hypotenuse. The longitude strain is determined by the hypotenuse as the stretched distance comparing to the unstretched distance. On the other hand, latitude strain is determined by stretched and unstretched distance along with latitude direction. The stretched distance along with latitude direction can be directly measured under two-dimensional image because two particles were located at the same level. Due to the axisymmetric character of the deformation, the strain distribution of a spherical cap at 15% deformation was characterized along with half a cross-section of spherical cap in Figure 3.

Cell culture

The human umbilical vein endothelial cell line EA.hy926 was maintained by our laboratory. EA.hy926 cells were routinely maintained in high-glucose DMEM (Gibco, USA) supplemented with 10% fetal bovine serum (FBS; PAA, Germany), penicillin ($100 \text{ U} / \text{mL}$, Gibco, USA) and streptomycin ($100 \mu\text{g} / \text{mL}$, Gibco, USA). The cells were cultured in a humidified environment containing 5% CO_2 at 37°C . After the confluence reached 70%–80% in culture dish, EA.hy926 cells were seeded into the stretching device.

Cell stretching

Prior to cell seeding, the device was sterilized in an autoclave at 121°C for 30 min and secured in a culture dish, then each well was thoroughly washed with the sterile phosphate-buffered saline (PBS) for three times. $25 \mu\text{g} / \text{mL}$ poly-D-lysine

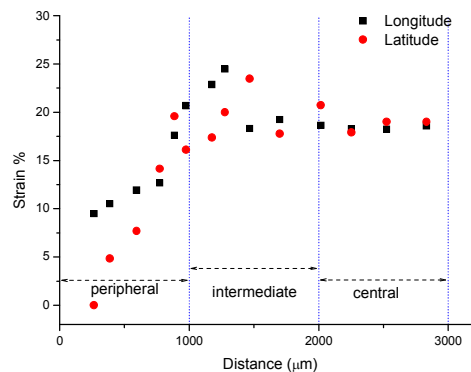


Figure 3. The distribution of longitude and latitude strains from edge to centre of a membrane (half of a cross-section). The strain is determined as the ratio of the distances between two points under the stretched (15%) and unstretched condition. The radius of the membrane is 3 mm and the height of the formed spherical cap is 1.16 mm.

(PDL; Beyotime, China) solution was added into the wells for coating overnight in an incubator with 5% CO_2 at 37°C . Next, about 7500 cells were seeded in each well and cultured at 5% CO_2 and 37°C for 36 h to ensure that cells proliferate at least one time. Before stretching, the culture medium was replaced by the serum-free DMEM. After that, the cyclic stretch was performed by the alternation between injection and suction at a frequency of 2.14 cycle / min. The cells cultured in the wells were subjected to the change of the intensity and duration of strain. The cells in the wells without stretched were used for the control. All stretching experiments were conducted at least in triplicate for quantitative analysis.

Cell viability assay

The cells were washed twice with PBS, followed by the incubation in the PBS containing three specific fluorescent probes, $2.5 \mu\text{g} / \text{mL}$ Calcein AM (Sigma, USA), $5 \mu\text{g} / \text{mL}$ Hoechst 33258 (Sigma, USA), and $5 \mu\text{g} / \text{mL}$ Propidium iodide (PI; Sigma, USA) for 20 min. The images were acquired by using an imaging system (Leica BMI 6000 inverted microscope, Germany) with LAF imaging software (Leica Microsystems, Inc., Germany).

RNA isolation and quantitative real-time PCR

Total RNA was extracted from EA.hy926 cells by using RNeasy Pure Micro Kit (TIANGEN, China). The samples were used to generate cDNA by using FastQuant RT kit with an oligo-dT primer (with gDNase; TIANGEN, China). Quantitative real-time PCR assays of MCP-1, IL-8, IL-6, ICAM-1, eNOS and Rel-A were performed by MX3000 real-time PCR instrument (Stratagene, USA) with Ultra SYBR Mixture (with ROX) (TIANGEN, China). Above procedures were recommended by the manufacturers. The designed primers used were shown in Table S-2 of the ESI. The $2^{-\Delta\Delta\text{CT}}$ method was used to analyze the relative quantification of each factor between the stretched and unstretched cells.

Western blotting assay

Proteins extracted from the cells used RIPA buffer (Beyotime, China) were separated by 10 % SDS-PAGE and transferred into PVDF membrane (Millipore, USA). Being blocked by 5 % non-fat milk in TBST, the membrane was incubated at 4 °C overnight with the primary antibodies, including GAPDH, MCP-1, ICAM-1, Rel-A and IL-8 (Proteintech, USA). After incubation, the membrane was washed with TBST for 3 × 10 min, and then incubated with the secondary antibody conjugated to horseradish peroxidase for 2 h at room temperature. The interested proteins were visualized by ECL (Advansta, USA) and detected using Bio-Rad ChemiDoc™ MP imaging system (Bio-Rad, USA).

Statistical Analysis

Data were showed as mean ± SD of at least three independent experiments. SPSS 17.0 software was used for all statistical analysis. Statistical differences among experimental groups were evaluated by one-way ANOVA *t*-test and student's *t*-test. *P* < 0.05 was considered to be statistically significance.

Results**The strain profile on the membrane**

Except for the axisymmetric character, the overall strains on entire spherical cap display somewhat heterogeneous. To better describe the strain profile on the formed spherical cap, the circle membrane is divided into three parts based on trisection of radius as the central, intermediate, and peripheral zones. Figure 3 shows that the strain profile across half a longitude line on the formed spherical cap (15 % deformation). Within the central zone, both of the longitude and latitude strain are approximately equal to 18 % with the equiaxial profile. Within the intermediate zone, in contrast, the longitude and latitude strains start to vary between about 15 % and 25 % while the longitude strains are larger than the latitude strains at the same location. Within the peripheral zone, however, both of the longitude and latitude strains keep decreasing toward the edge of the membrane, but the decline rate of the latitude strain is larger than that of the longitude strain.

Furthermore, the stretching consistence of the device was evaluated by measuring the height of each formed spherical cap in a set of the wells. As can be seen in Table 1, the relative standard deviations (RSD) of the heights are below 8.9 % at 5 % deformation and above 2.6 % at 20 % deformation. With the same degree of deformation, both the height and the stretching consistence (RSD) at the beginning of the stretch are comparable to those after 24 h stretch. The Table 1 demonstrates the stretching consistence of the device is satisfactory for the use within 24 hour and even longer.

Cellular responses to the strains

Cell morphology. Figure 4 shows the generally morphological behaviours of the cells under the different stretch conditions and classified regions. As shown in Figure 4A, after 6 hour stretch, the cells protrude two or three antennas in order to connect around cells. This tendency was more prominent with increasing the deformation from 5 % to 20 %. Because of the equiaxial and heterogeneous profile of the strains in the central and intermediate regions, the orientation response of the cells there to stretch did not shown obviously preferred direction. However, in peripheral regions, the orientation of the cells showed somewhat perpendicular to longitude direction. After stretched for 12 h, in contrast, the cells shrink down to round balls more prominently with the increment of the degree of the deformation (Figure 4B). It is very different from the situation of the cells after applying stretch for 6 h, where the most cells exhibited omnidirectional attachment with spindle or triangular shape. This phenomenon provides an evident for the morphological change of endothelial cells under the nonuniform strain profile. The vascular endothelium could tend to be penetrable under the higher strength of nonuniform strains. It might be a contributor to vascular diseases.

Cell viability. After applying stretch for 6 h, the majority of the cells were stained with Calcium AM without showing the obvious effect of the degree of the deformation on the cell viability. In contrast, after applying stretch for 12 h, the more cells were stained with Hoechst and PI with increasing the degree of the deformation. Figure 5A and 5B shows the representative 200 × images of the cells cultured within the central regions after applying the stretch for 6 h and 12 h, respectively. The similar results could be found for the cells stretched within the intermediate regions. However, the cells within the peripheral regions exhibited less apoptotic rates than those within the central and intermediate regions under same degree of the deformation (shown in Figure S-2 of the ESI). Figure 6 indicates the rate of cell apoptosis is in response to the different stretch conditions. Compared with other regions, the apoptotic rate of the cells within the peripheral regions remained relatively low because the locate strains were uniaxial-dominated with decreasing magnitude. On the other hand, within the central and intermediate regions the apoptotic rates of the cells of 12 h stretch group were seen significantly increased with increasing the degree of the deformation. Moreover, the images of the cells stained by Hoechst and PI overlap each other to suggest that the cell death is related to the cell apoptosis in these experiments.

Table 1 The variation of the height of the spherical cap formed in each well of the device (5x5)

*Degree of the deformation	At the beginning of the stretch		After 24 h stretch	
	Averaged height (mm, n = 5)	RSD %	Averaged height (mm, n = 5)	RSD %
5 %	0.660	7.7	0.635	8.9
10 %	0.870	4.9	0.853	5.1
15 %	1.230	2.2	1.203	2.5
20 %	1.333	3.6	1.315	2.6

* The degrees of the deformation were not calibrated.

Proinflammatory gene and protein expression. The inflammation induced by a variety of stimuli is one of the key events in the initial development of cardiovascular diseases. To demonstrate the ability of this device to induce the inflammatory responses

of EA. hy926 cells, the mRNA and protein expressions of the relevant proinflammatory cytokines were detected, such as MCP-1, IL-8, IL-6, eNOS, ICAM-1 and Rel-A (Figure 7).

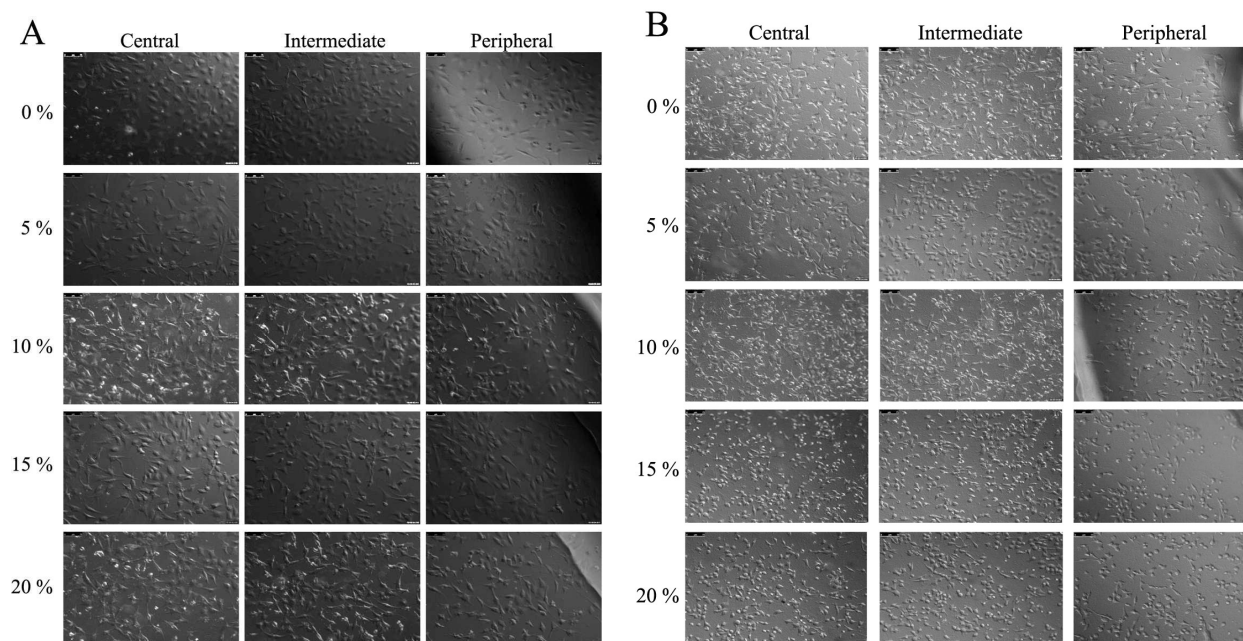


Figure 4. The images (20× objective) of cellular morphology were captured after 6 h (A) and 12 h (B) stretch. Note: Four lines of each set of the images were captured under the different degrees of the deformation at 0% (unstretched), 5%, 10%, 15%, and 20%, respectively; three columns of each set of images were captured at the central, intermediate and peripheral regions, respectively. The scale bar is 75 μm (up left corner).

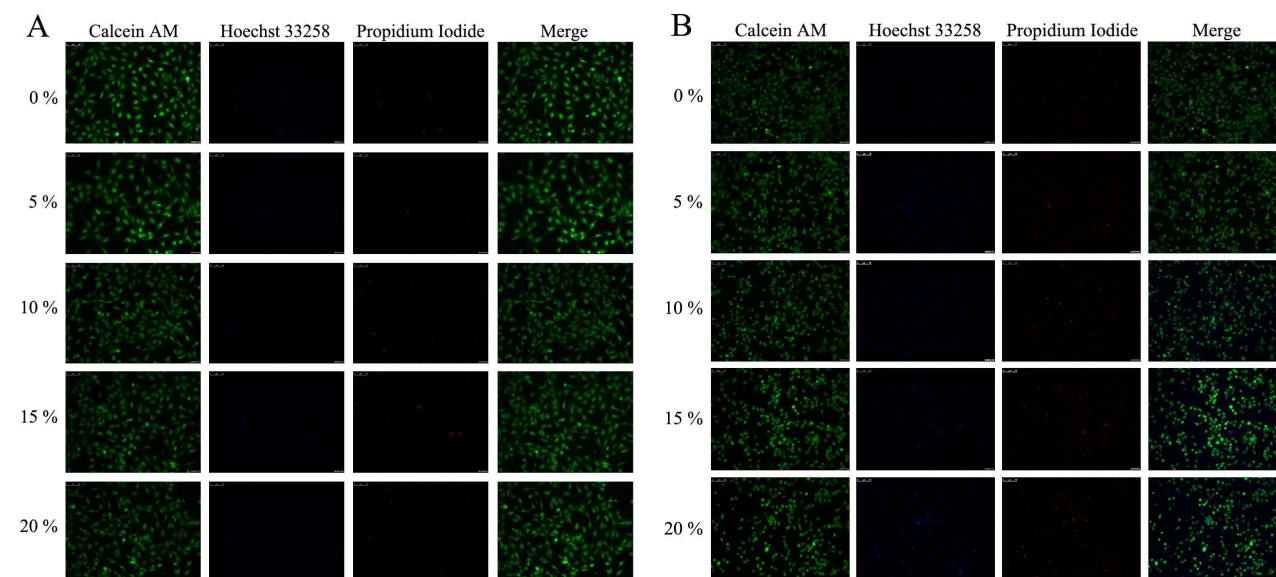


Figure 5. Fluorescent images (20× objective) of the cells in the central regions of the well bottoms under the different degrees of the deformation for 6 h (A) and 12 h (B). The scale bar is the same as in Figure 4.

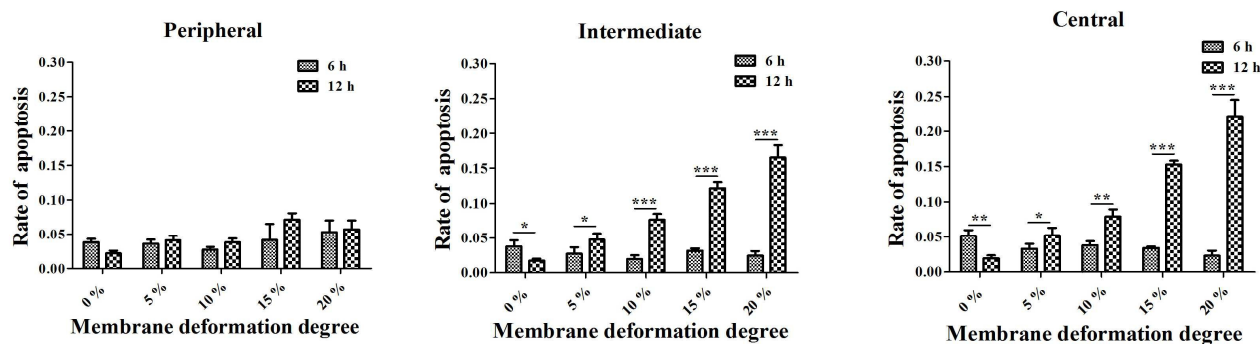


Figure 6. Effect of the degree of the deformation on the apoptotic rate of the cells in the different regions. Error bars represented mean \pm SD of triplicates (* P <0.05, ** P <0.01, and *** P <0.001).

As shown in Figure 7A, the mRNA expressions of the proinflammatory factors exhibited moderate variation in 6 h stretch group compared with the control group. When the degree of the deformation increased, the mRNA expressions of MCP-1 and ICAM-1 showed slightly upregulated. In contrast, the mRNA expression of IL-8 showed significantly down-regulated under the stretch conditions from 10 to 20% deformation. As can be seen in Figure 7B for 12 h stretch, the mRNA expressions of MCP-1, IL-6, and IL-8 exhibited significantly upregulated at the higher degrees of the deformation. The mRNA expression of eNOS was down-regulated at the degree of the deformation above 10%. Differently, the mRNA expression of ICAM-1 only showed an identified increment at 15% deformation. The mRNA expression of Rel-A did not show any significant changes either in 6 h or 12 h stretch groups.

The western blots were performed to further confirm the inflammatory response induced by the use of this device. The protein expressions of four factors, including Rel-A, MCP-1, IL-8, and ICAM-1, were shown in Figure 7 C and D. The expressions of these proteins were similar to the corresponding mRNA expressions. The results suggest that large strain can induce inflammatory responses of EA. hy926 cell. However, the levels of these protein expressions were relatively low at 20% deformation compared with 15% deformation. This might be explained that cells inclined to detach from substrate to diminish stretch stimuli when strain became large.

Discussion

Currently, most of stretching devices only provide uniaxial or equibiaxial strain to cells on flat surface.

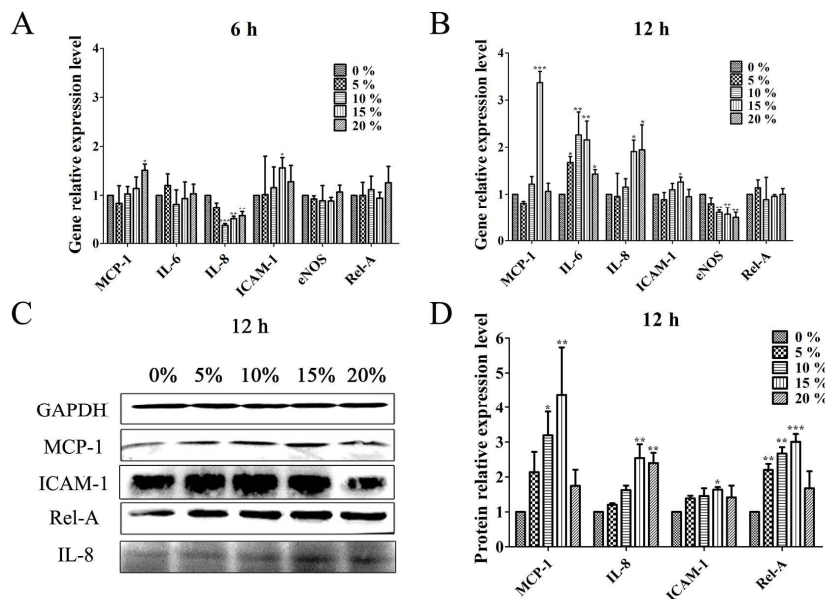


Figure 7. The mRNA and protein expressions of some inflammatory factors under the different degrees of the deformation. The mRNA expressions for 6 h stretch (A) and 12 h stretch (B). Western blotting images (C) and histograms (D) of the protein expression for 12 h stretch compared with the control (unstretched). Error bars represented mean \pm SD of triplicates, * P <0.05, ** P <0.01, and *** P <0.001.

Differently, our device here provides a three-dimension deformation based on the formation of a spherical cap, where endothelial cells are subjected to similar strain stimuli at the bending area of blood vessels. To facilitate the description of this strain profile, the membrane (well bottom) was divided into the central, intermediate, peripheral regions according to the separation of the radius into three equal parts. As revealed in Figure 3, the strain distribution was heterogeneous and roughly classified into three distinctive profiles. In the central region, the longitude and latitude strain was approximately equal each other. However, in the intermediate region, the two types of strain became uneven and fluctuant, and also both of them tended to be larger than the strains in the central region. In the peripheral region, due to the boundary effect of the membrane, both the latitude and longitude strain was limited and decreased toward the edge. Furthermore, the latitude strain decreased more quickly than the longitude strain, resulting in the longitude strain was dominant in the peripheral region. This overall strain profile is likely to mimic the stretching stimuli at the curvatures of blood vessels, where lesion is easy to occur.

It is well documented that cells undergo morphological transform in response to uniaxial stretch by arranging elongated cells perpendicular to stretching direction. However, the situations of cells responding to non-uniform and omnidirectional strain profile are rarely reported. As depicted in Figure 4, after stretched for 6 h, the cells became elongated with long pseudopodium to contact the around cells; however, the orientation of the cells did not show obviously preferred direction except those cells in the peripheral region. On the other hand, after stretched for 12 h, the cells turned to be round up in response to this complicated strains. This phenomenon may be related to some adaptive responses which resisted highly mechanical stimuli. This trend of cell detachment also implied that the permeability of endothelium is more easily to occur at bending and branch vessels than straight vessels.

To assess the effect of the different degrees of the deformation on the cell viability, the stretched cells were stained with three fluorescent dyes. The living, apoptotic, dead cells were stained green, blue, and red with Calcein AM, Hoechst 33258, and PI, respectively. Due to the limitation of cell number in a small culture wells, the dye staining is a straight method to evaluate cell viability in this experiment (Figure 5). Using this stretching device, the cells stretched for 6 h under no matter low or high degree of the deformation showed little effect of the strain on the cell viability. However, after stretched for 12 h, the cell viability was affected significantly under the higher degree of the deformation. In the central region, the apoptotic rate of cell was significantly increased up to more than 15 % and 20 % under 15 % and 20 % deformation, respectively. In contrast, the apoptotic rates of cell were low in the peripheral region, since the overall strains

6 N. Scuor, P. Gallina, H. V. Panchawagh, R. L. Mahajan, O. Sbaizero and V. Sergo, *Biomed Microdevices*, 2006, 8, 239-246.

are relatively low even at high degree of the deformation (Figure 6).

In Figure 7, the change in the mRNA and protein expression of the proinflammatory factors demonstrated the occurrence of the inflammation response in the cells. MCP-1 and IL-8 act as the key role for recruitment of monocytes and neutrophils, respectively. Their expressions both in mRNA and protein level significantly increased with enlarging the degree of the deformation. The fact of the overexpression of IL-6 mRNA may stimulate acute phase protein synthesis and promote development of inflammation. Meanwhile, since the low expression of eNOS mRNA is related to the progression of the inflammation, it was downregulated with increasing the degree of the deformation. The mRNA expressions of ICAM-1 and Rel-A showed slightly change at different degrees of the deformation, but their protein expressions were upregulated with increasing the degree of the deformation. Based on above PCR and western blotting experiments, these non-uniform and axisymmetric strains were demonstrated to induce cell inflammatory responses.

Conclusions

Using this multi-well stretching device, the non-uniform strains in each well was generated through changing surface area of spherical cap. The obtained results demonstrate that the inflammatory responses of EA.hy926 cells can be induced based on this stretching device. Compared to macro stretching devices, this device provides the three-dimension strain profile to mimic in vitro complex strain profile at bending site of blood vessels. On the other hand, this device provides the ability to conduct mRNA and protein expression experiments other than only morphological observation by micro stretching devices. Additionally, this device also exhibits extra merits, such as easy-to-do, low cost and simple instrumentation.

Acknowledgements

This work was supported partly by the CAS/SAFEA International Partnership Program for Creative Research Teams and the National Natural Sciences Foundation of China (21075135). The authors have declared no conflict of interest.

Notes and references

- 1 J. J. Chiu and S. Chien, *Physiol Rev*, 2011, 91, 327-387.
- 2 J. Ando and K. Yamamoto, *Antioxid Redox Signal*, 2011, 15, 1389-1403.
- 3 J. C. Choy, D. J. Granville, D. W. Hunt and B. M. McManus, *J Mol Cell Cardiol*, 2001, 33, 1673-1690.
- 4 C. P. Ursekar, S. K. Teo, H. Hirata, I. Harada, K. H. Chiam and Y. Sawada, *PLoS One*, 2014, 9, e90665.
- 5 S. P. Arold, J. Y. Wong and B. Suki, *Ann Biomed Eng*, 2007, 35, 1156-1164.
- 6 W. J. Richardson, R. P. Metz, M. R. Moreno, E. Wilson and J. E. Moore, Jr., *J Biomech Eng*, 2011, 133, 101008.
- 7 T. A. Lusardi, J. Rangan, D. Sun, D. H. Smith and D. F. Meaney, *Ann Biomed Eng*, 2004, 32, 1546-1558.

Paper

Lab on a Chip

- 9 P. Lacolley, *Cardiovascular Research*, 2004, 63, 577-579.
- 10 A. Quaglino, M. Salierno, J. Pellegrotti, N. Rubinstein and E. C. Kordon, *BMC Cell Biol*, 2009, 10, 55.
- 11 V. Mukundan, W. J. Nelson and B. L. Pruitt, *Biomed Microdevices*, 15, 117-123.
- 12 D. Tremblay, S. Chagnon-Lessard, M. Mirzaei, A. E. Pelling and M. Godin, *Biotechnol Lett*, 2014, 36, 657-665.
- 13 P. J. McMahon, S. Chow, L. Sciaroni, B. Y. Yang and T. Q. Lee, *J Rehabil Res Dev*, 2003, 40, 349-359.
- 14 J. Imsirovic, K. Derricks, J. A. Buczek-Thomas, C. B. Rich, M. A. Nugent and B. Suki, *Biomatter*, 3.
- 15 Y. Huang and N. T. Nguyen, *Biomed Microdevices*, 2013, 15, 1043-1054.
- 16 J. M. Mann, R. H. Lam, S. Weng, Y. Sun and J. Fu, *Lab Chip*, 2012, 12, 731-740.
- 17 L. Huang, P. S. Mathieu and B. P. Helmke, *Ann Biomed Eng*, 2010, 38, 1728-1740.
- 18 Y. Shao, X. Tan, R. Novitski, M. Muqaddam, P. List, L. Williamson, J. Fu and A. P. Liu, *Rev Sci Instrum*, 2013, 84, 114304.
- 19 R. D. Gregory, T. I. Milac and F. Y. M. Wan, *Studies in Appl. Math*, 1998, 100, 67-94.